European Conference on Optical Communication (ECOC) 2022 © Optica Publishing Group 2022

Plasmonic 100-GHz Electro-Optic Modulators for Cryogenic Applications

Patrick Habegger[1,2], Yannik Horst[2], Stefan M. Koepfli[2], Manuel Kohli[2], Eva De Leo[1], Dominik Bisang[2], Marcel Destraz[1], Valentino Tedaldi[1], Norbert Meier[1], Nino Del Medico[1], Wei Wang[1,2], Claudia Hoessbacher[1], Benedikt Baeuerle[1], Wolfgang Heni[1], and Juerg Leuthold[1,2]

[1] Polariton Technologies AG, 8803 Rüschlikon, Switzerland, patrick.habegger@polariton.ch
[2] ETH Zurich, Institute of Electromagnetic Fields (IEF), 8092 Zurich Switzerland

Abstract *We demonstrate an energy-efficient, 100-GHz plasmonic modulator operating at 4 K for beyond 128 GBd data modulation with ultra-low driving voltage of 0.1 V. High-speed components at cryogenic temperature are essential building blocks for scalable next-generation quantum computing systems. ©2022 The Author(s)*

Introduction

High-speed modulators operating in cryogenic environments are essential to operate next-generation superconducting quantum circuits. To avoid excessive heat dissipation only devices meeting the most stringent lowest-power requirements can be used [1].

Complexity of cryogenic circuits is steadily increasing [2-4]. Accordingly, the respective communication interfaces scale equally. Here, optical solutions can offer lower heat load and higher bandwidth over their electrical counterpart. Increasingly, electro-optical interfaces operating at cryogenic temperatures below 4 K are introduced to the community [1, 5-7]. For instance, by using a commercial 5-GHz lithium niobate modulator data rates of 5 Gbit/s were demonstrated in the mK regime [1]. More recently, barium titanate modulators offering a 30-GHz electro-optic bandwidth have been demonstrated at 20 Gbit/s with a 0.85 V_P drive voltage [5]. Other examples include the silicon spoked-ring modulator [7] or graphene-based ring modulators [6] that have demonstrated operation with similar data rates and operation voltages. In general, a modulator is characterized by its $V_\pi L$ product. This means that a lower voltage can be traded in against a lower length. Yet, a longer modulator length comes at the price of lower bandwidth. So, while the above prior art show very promising results, reaching higher speed remains a challenge.

A promising alternative to existing cryogenic electro-optic interfaces are plasmonic modulators. For classical applications, this technology has already demonstrated a combination of highest-bandwidth (>500 GHz [8]), performance (222 GBd symbol rate [9]), energy efficiency (driving voltage <100 $\mathrm{mV_P}$ [10]), and low-loss (1.0 dB on-chip losses [11]).

In this paper, we demonstrate that plasmonic modulators are promising candidates for cryogenic electro-optic interfaces in quantum systems. We show an electro-optic bandwidth of >100 GHz, 128 GBd high-speed data transmission with sub-500 $\mathrm{mV_P}$ drive voltages. Furthermore, 16 GBd operation is shown with low electrical driving voltages of sub 100 $\mathrm{mV_P}$, removing the need for electrical amplifiers in cryostats. Furthermore, we demonstrate for the first time that organic electro-optical materials in plasmonic modulators operate reliably and efficiently in cryogenic environments. All measurements were performed in a closed-loop liquid-helium cryostat at a base temperature of 3.2 K.

Device Design & Cryogenic Characterization

The cryogenic device consists of a plasmonic Mach-Zehnder modulator operated in push-pull mode. The schematic of the device is depicted in Fig. 1(a). It features plasmonic phase shifters in the two arms, each with a slot width of 130 nm

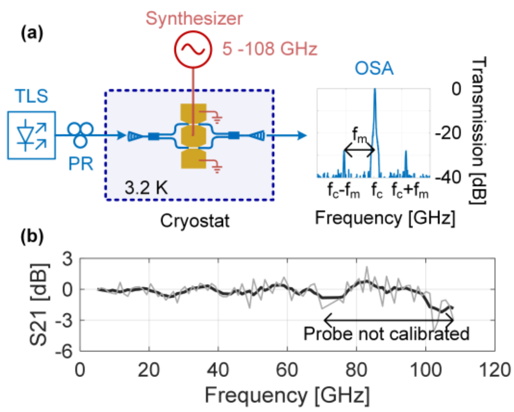

Fig. 1: (a) Schematic drawing of the experimental setup for the MZM bandwidth measurement with an optical spectrum at 70 GHz small-signal RF modulation. (b) Measured and normalized electro-optical frequency response of the plasmonic MZM.

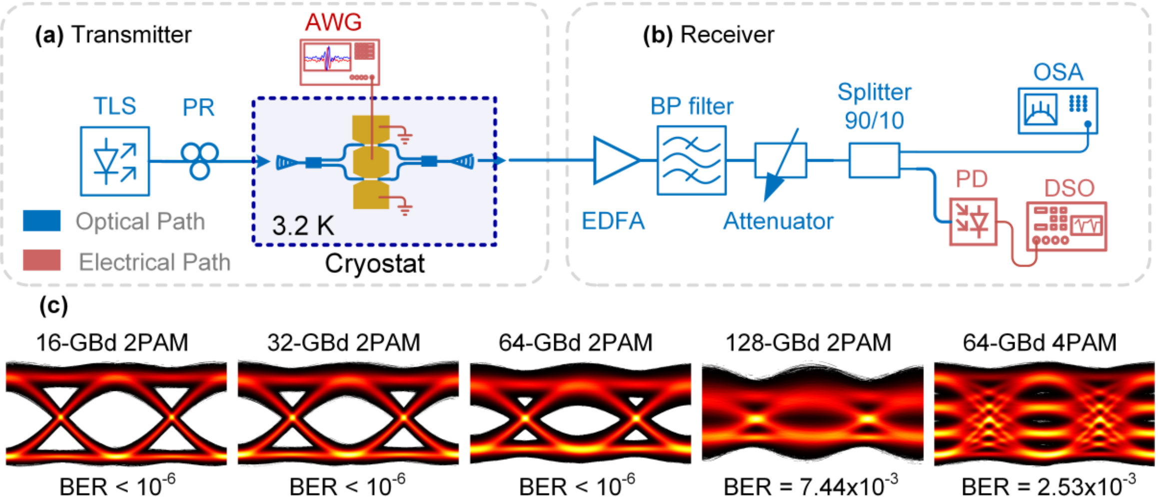

Fig. 2: Schematic illustration of the experimental setup for data measurements and eye diagrams. (a) Simplified drawing of the transmitter. No electrical amplifiers were used to drive the modulator located in the cryogenic chamber. (b) Receiver used for the data transmission experiments. (c) Recorded eye-diagrams for transmitted PAM2 and PAM4 signals.

and a length of 15 µm. Optical coupling to the photonic integrated circuit (PIC) chip is achieved via grating couplers. To facilitate optical alignment, a fiber array (FA) was glued to the PIC using cryo-compatible epoxy. The MZM features an imbalance between the two arms introducing a fixed phase shift. This allows to adjust the modulator operating point without the need for electrical tuning, e.g. by a thermo-optic phase shifter, avoiding additional thermal load to the cryostat. The phase modulation is achieved exploiting the linear electro-optic effect (quantified by the electro-optic coefficient r_{33}) of an organic electro-optic (OEO) material [12]. OEO materials have been demonstrated to exhibit high nonlinearities down to 4.2 K [13]. The in-device nonlinearity in this work was determined to be r_{33} = 159 pm/V, measured at RT.

The device was characterized for its frequency response at RT and in a 4 K environment. Fig. 1(a) depicts the characterization setup. Fig 1(b) shows the near to flat frequency response from 5 GHz up to 108 GHz at 4 K. More precisely, the sample has been placed inside a 4 K closed-loop liquid-helium cryostat. A temperature sensor installed on top of the sample stage has measured the temperature close to the chip. The PIC chip was kept at 3.2 K for > 12 h prior to each experiment, to ensure steady-state temperature. A 1532.5 nm optical carrier from a tuneable laser source (TLS) has been connected to the device under test (DUT). The operation point of the modulator was set to its quadrature point (3-dB point). To determine the electro-optic response, an electrical sinusoidal signal (5–108 GHz) was fed to the modulator via a 67-GHz vacuum RF feedthrough and a RF probe. The signal has been generated with help of a synthesizer for frequencies up to 70 GHz and for frequencies beyond with an additional multiplier. The electrical losses of the setup (excluding the prober needle) was characterized at room temperature using an electrical spectrum analyser and taken into account for the calibration. The modulated output signal of the MZM was recorded using an optical spectrum analyser (OSA). It should be stressed that a 67-GHz probe was utilized for the measurements that was calibrated for up to 67 GHz. For higher frequency, the calibration has been normalized to the loss at the 67 GHz value. The more pronounced oscillations beyond 67 GHz can very likely be explained by the uncalibrated probe needle. The measured average frequency as indicated by the black solid line shows a 108 GHz frequency response with -2.2 dB drop.

The on-off voltage V_π was measured both at RT and in a 4 K environment using a 100 kHz signal. $V_{\pi,50\Omega}$ increased from 3.3 V at RT to 4.2 V at 4 K. This decrease in modulation efficiency could arise from temperature-related stress in the setup and needs further investigation.

Cryogenic Data-Transmission Experiments

We test the electro-optic interface for high-speed data modulation, and later we investigate the influence of reduced electrical drive voltages. In order to verify high-speed data extraction from the cryostat, the plasmonic modulator is operated at data rates up to 128 Gbit/s. In these experiments, data is generated outside of the cryostat and is fed-in using 67 GHz RF feedthroughs, imposing additional RF impairments. The transmitter is operated as described in the previous section, see Fig. 2(a).

European Conference on Optical Communication (ECOC) 2022 © Optica Publishing Group 2022

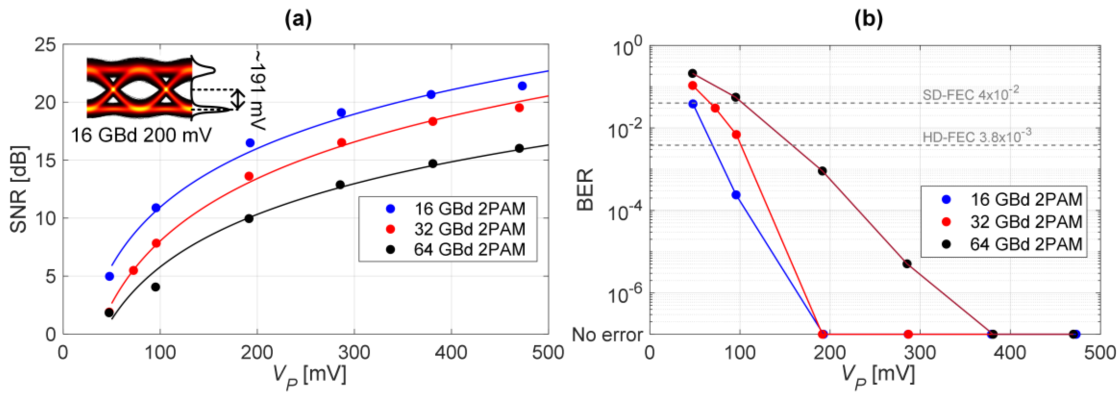

Fig. 3: Electrical drive voltages to operate the MZM measured in 4 K environment. (a) Measured SNR of 16 – 64 GBd 2PAM signals as a function of the applied peak voltage V_P. The eye diagram for a 16 GBd signal with nominal electrical V_P driving voltage of 200 mV is shown as an inset. (b) BER after applying timing recovery (TR) and least-mean square error correction (LMS). The HD-FEC and SD-FEC limits are indicated by dashed grey lines.

The varying data formats are generated using a 256 GSa/s, 70-GHz arbitrary waveform generator (AWG) with an electrical driving voltage chosen such that $V_{P,50\Omega}$ is below 500 mV. At the receiver, see Fig. 2(b), the modulated optical output signal was amplified using an erbium-doped fiber amplifier (EDFA) and filtered, before feeding 90% of the signal into a 145 GHz photodiode (PD) connected to a digital sampling oscilloscope (DSO) for offline digital signal processing (DSP). 10 % of the amplified and filtered signal is monitored using an OSA. The DSP consists of a matched filter, a timing recovery and static T/2-spaced feed-forward equalizer that has been trained by a data-aided least mean square with 99 filter taps. The eye diagrams of the recorded data transmission with 16 – 128 GBd 2PAM (128 Gbit/s) and 64 GBd 4PAM (128 Gbit/s) signals are shown in Fig. 2(c). The transmission of 10^6 symbols remained error-free up to 64 GBd 2PAM. Furthermore, Fig. 3 shows the digitally calculated SNR and the BER for 2PAM signals for varied electrical driving voltage and data rates, indicating that a low driving voltage of 0.1 $V_{P,50\Omega}$ can support a 16 Gbd 2PAM signal below the SD-FEC limit [14]. For $V_{P,50\Omega}$ as low as 200 mV, transmission of $5\text{x}10^5$ symbols lead to error-free communication for symbol rates of 16 GBd and 32 GBd, while BER of the 64 GBd signal remains below the HD-FEC limit [15].

This work shows that the plasmonic modulators are well suited for demanding cryogenic applications featuring highly efficient EO conversion even at temperatures < 4 K. Improvements in the measurement setup should lead to even better performance. Taking into account the small difference of the performance between RT and 4 K environment in this demonstration, we expect that room temperature experiments can be directly translated to the cryogenic environment. This way, cryogenic high-speed operation up to 432 Gbit/s in 8PAM [16] with 1.0 dB on-chip IL [11] should be feasible.

Conclusions

We demonstrate for the first time an integrated plasmonic modulator at cryogenic temperatures for quantum system applications. The plasmonic modulators feature electro-optical bandwidths in excess of 100 GHz in a < 4K cryogenic environment. Furthermore, we have demonstrated high-speed data transmission with up to 128 GBd 2PAM signals in a 4 K environment without electrical amplifiers and low electrical drive signals of 200 $\mathrm{m}V_{P,50\Omega}$ at data rates of 64 Gbit/s and 100 $\mathrm{m}V_{P,50\Omega}$ at data rates of 16 Gbit/s.

Acknowledgements

This work was supported by the European Union's Horizon 2020 Research and Innovation Program through the project aCryComm, FET Open Grant Agreement no. 899558. We thank the Cleanroom and Operations team of the Binning and Rohrer Nanotechnology Center (BRNC) for their support. Polariton Technologies acknowledges NLM Photonics for providing the organic electro-optic material. The free and open-source laboratory automation software LabExT has been used to conduct the measurements in this study.

Disclaimer: Preliminary paper, subject to publisher revision

References

[1] A. Youssefi, I. Shomroni, Y. J. Joshi, N. R. Bernier, A. Lukashchuk, P. Uhrich, L. Qiu, and T. J. Kippenberg, "A cryogenic electro-optic interconnect for superconducting devices," *Nature Electronics,* vol. 4, pp. 326-332, 2021/05/01 2021.

[2] S. Krinner, S. Storz, P. Kurpiers, P. Magnard, J. Heinsoo, R. Keller, J. Luetolf, C. Eichler, and A. Wallraff, "Engineering cryogenic setups for 100-qubit scale superconducting circuit systems," *EPJ Quantum Technology,* vol. 6, p. 2, 2019.

[3] F. Arute, K. Arya, R. Babbush, D. Bacon, J. C. Bardin, R. Barends, R. Biswas, S. Boixo, F. G. Brandao, and D. A. Buell, "Quantum supremacy using a programmable superconducting processor," *Nature,* vol. 574, pp. 505-510, 2019.

[4] H. Riel, "Quantum Computing Technology," in *2021 IEEE International Electron Devices Meeting (IEDM)*, 2021, pp. 1.3. 1-1.3. 7.

[5] F. Eltes, G. E. Villarreal-Garcia, D. Caimi, H. Siegwart, A. A. Gentile, A. Hart, P. Stark, G. D. Marshall, M. G. Thompson, and J. Barreto, "An integrated optical modulator operating at cryogenic temperatures," *Nature Materials,* vol. 19, pp. 1164-1168, 2020.

[6] B. S. Lee, B. Kim, A. P. Freitas, A. Mohanty, Y. Zhu, G. R. Bhatt, J. Hone, and M. Lipson, "High-performance integrated graphene electro-optic modulator at cryogenic temperature," *Nanophotonics,* vol. 10, pp. 99-104, 2021.

[7] H. Gevorgyan, A. Khilo, D. Van Orden, D. Onural, B. Yin, M. T. Wade, V. M. Stojanović, and M. A. Popović, "Cryo-Compatible, Silicon Spoked-Ring Modulator in a 45nm CMOS Platform for 4K-to-Room-Temperature Optical Links," in *2021 Optical Fiber Communications Conference and Exhibition (OFC)*, 2021, pp. 1-3.

[8] M. Burla, C. Hoessbacher, W. Heni, C. Haffner, Y. Fedoryshyn, D. Werner, T. Watanabe, H. Massler, D. L. Elder, and L. R. Dalton, "500 GHz plasmonic Mach-Zehnder modulator enabling sub-THz microwave photonics," *Apl Photonics,* vol. 4, p. 056106, 2019.

[9] W. Heni, B. Baeuerle, H. Mardoyan, F. Jorge, J. M. Estaran, A. Konczykowska, M. Riet, B. Duval, V. Nodjiadjim, and M. Goix, "Ultra-high-speed 2: 1 digital selector and plasmonic modulator IM/DD transmitter operating at 222 GBaud for intra-datacenter applications," *Journal of Lightwave Technology,* vol. 38, pp. 2734-2739, 2020.

[10] B. Baeuerle, W. Heni, C. Hoessbacher, Y. Fedoryshyn, U. Koch, A. Josten, T. Watanabe, C. Uhl, H. Hettrich, D. L. Elder, L. R. Dalton, M. Möller, and J. Leuthold, "120 GBd plasmonic Mach-Zehnder modulator with a novel differential electrode design operated at a peak-to-peak drive voltage of 178 mV," *Optics Express,* vol. 27, pp. 16823-16832, 2019/06/10 2019.

[11] M. Eppenberger, B. I. Bitachon, A. Messner, W. Heni, D. Moor, L. Kulmer, P. Habegger, M. Destraz, E. De Leo, and N. Meier, "Enhanced Stability of Resonant Racetrack Plasmonic-Organic-Hybrid Modulators," in *Optical Fiber Communication Conference*, 2022, p. Th3C. 3.

[12] H. Xu, F. Liu, D. L. Elder, L. E. Johnson, Y. de Coene, K. Clays, B. H. Robinson, and L. R. Dalton, "Ultrahigh electro-optic coefficients, high index of refraction, and long-term stability from Diels–Alder cross-linkable binary molecular glasses," *Chemistry of Materials,* vol. 32, pp. 1408-1421, 2020.

[13] D. Park, V. Yun, X. Zhou, J. Luo, A.-Y. Jen, and W. Herman, "Cryogenic optical characterization of nonlinear polymers," in *CLEO/QELS: 2010 Laser Science to Photonic Applications*, 2010, pp. 1-2.

[14] K. Schuh, F. Buchali, W. Idler, T. A. Eriksson, L. Schmalen, W. Templ, L. Altenhain, U. Dümler, R. Schmid, and M. Möller, "Single carrier 1.2 Tbit/s transmission over 300 km with PM-64 QAM at 100 GBaud," in *Optical Fiber Communication Conference*, 2017, p. Th5B. 5.

[15] J. Cho, C. Xie, and P. J. Winzer, "Analysis of soft-decision FEC on non-AWGN channels," *Optics Express,* vol. 20, pp. 7915-7928, 2012/03/26 2012.

[16] Q. Hu, R. Borkowski, Y. Lefevre, F. Buchali, R. Bonk, K. Schuh, E. De Leo, P. Habegger, M. Destraz, and N. Del Medico, "Plasmonic-MZM-based Short-Reach Transmission up to 10 km Supporting> 304 GBd Polybinary or 432 Gbit/s PAM-8 Signaling," in *2021 European Conference on Optical Communication (ECOC)*, 2021, pp. 1-4.